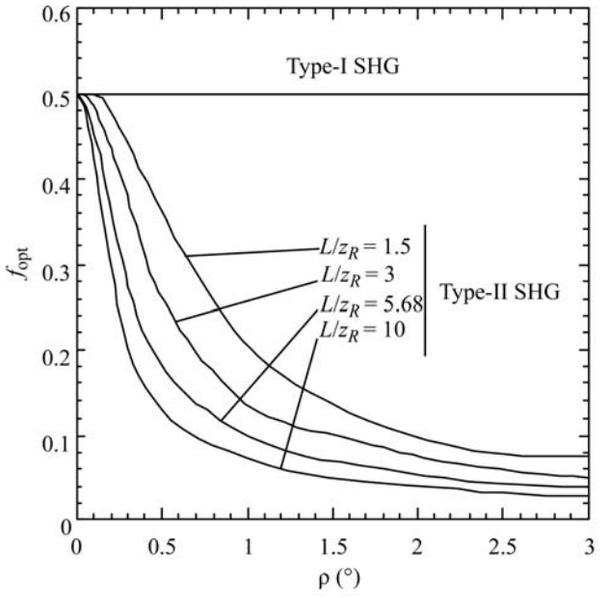

Fig. 1.7.3.12. Position f_{opt} of the beam waist for different values of walk-off angles and L/z_R, leading to an optimum SHG conversion efficiency. The value $f_{opt} = 0.5$ corresponds to the middle of the crystal and $f_{opt} = 0$ corresponds to the entrance surface (Fève & Zondy, 1996).

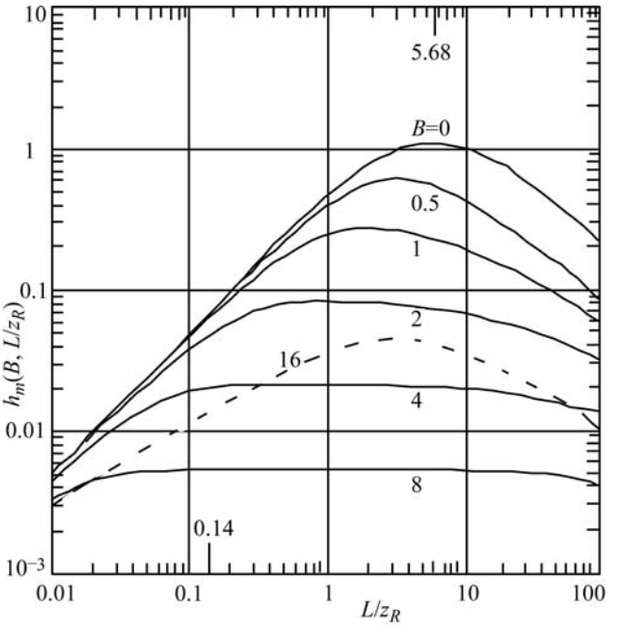

Fig. 1.7.3.13. Optimum walk-off function $h_m(B, L)$ as a function of L/z_R for various values of $B = (1/2)\rho\{[(k_o^\omega + k_e^\omega)/2]L\}^{1/2}$. The curve at $B = 0$ is the same for both type-I and type-II phase matching. The full lines at $B \neq 0$ are for type II and the dashed line at $B = 16$ is for type I. (From Zondy, 1990).

The computation of $h(L, w_o, \rho, f, \Delta k)$ allows an optimization of the SHG conversion efficiency which takes into account L/z_R, the waist location f inside the crystal and the phase mismatch Δk.

Fig. 1.7.3.12 shows the calculated waist location which allows an optimal SHG conversion efficiency for types I and II with optimum phase matching. From Fig. 1.7.3.12, it appears that the optimum waist location for type I, which leads to an optimum conversion efficiency, is exactly at the centre of the crystal, $f_{opt} = 0.5$. For type II, the focusing (L/z_R) is stronger and the walk-off angle is larger, and the optimum waist location is nearer the entrance of the crystal. These facts can be physically understood: for type I, there is no walk-off for the fundamental beam, so the whole crystal length is efficient and the symmetrical configuration is obviously the best one; for type II, the two fundamental rays can be completely separated in the waist area, which has the strongest intensity, when the waist location is far from the entrance face; for a waist location nearer the entrance, the waist area can be selected and the enlargement of the beams from this area allows a spatial overlap up to the exit face, which leads to a higher conversion efficiency.

The divergence of the pump beam imposes non-collinear interactions such that it could be necessary to shift the direction of propagation of the beam from the collinear phase-matching direction in order to optimize the conversion efficiency. This leads to the definition of an optimum phase-mismatch parameter Δk_{opt} $(\neq 0)$ for a given L/z_R and a fixed position of the beam waist f inside the crystal.

The function $h(L, w_o, \rho, f_{opt}, \Delta k_{opt})$, written $h_m(B, L)$, is plotted in Fig. 1.7.3.13 as a function of L/z_R for different values of the walk-off parameter, defined as $B = (1/2)\rho\{[(k_o^\omega + k_e^\omega)/2]L\}^{1/2}$, at the optimal waist location and phase mismatch.

Consider first the case of angular NCPM $(B = 0)$ where type-I and -II conversion efficiencies obviously have the same L/z_R evolutions. An optimum focusing at $L/z_R = 5.68$ exists which defines the optimum focusing $z_{R_{opt}}$ for a given crystal length or the optimal length L_{opt} for a given focusing. The conversion efficiency decreases for $L/z_R > 5.68$ because the increase of the 'average' beam radius over the crystal length due to the strong focusing becomes more significant than the increased peak power in the waist area.

In the case of angular CPM $(B \neq 0)$, the L/z_R variation of type-I conversion efficiency is different from that of type II. For type I, as B increases, the efficiency curves keep the same shape, with their maxima abscissa shifting from $L/z_R = 5.68$ $(B = 0)$ to 2.98 $(B = 16)$ as the corresponding amplitudes decrease. For type II, an optimum focusing becomes less and less appearent, while $(L/z_R)_{opt}$ shifts to much smaller values than for type I for the same variation of B; the decrease of the maximum amplitude is stronger in the case of type II. The calculation of the conversion efficiency as a function of the crystal length L at a fixed z_R shows a saturation for type II, in contrast to type I. The saturation occurs at $B \simeq 3$ with a corresponding focusing parameter $L/z_R \simeq 0.4$, which is the limit of validity of the parallel-beam approximation. These results show that weak focusing is suitable for type II, whereas type I allows higher focusing.

The curves of Fig. 1.7.3.14 give a clear illustration of the walk-off effect in several usual situations of crystal length, walk-off angle and Gaussian laser beam. The SHG conversion efficiency is calculated from formula (1.7.3.56) and from the function (1.7.3.57) at f_{opt} and Δk_{opt}.

1.7.3.3.2.3. *Non-resonant SHG with depleted pump in the parallel-beam limit*

The analytical integration of the three coupled equations (1.7.3.22) with depletion of the pump and phase mismatch has only been done in the parallel-beam limit and by neglecting the walk-off effect (Armstrong *et al.*, 1962; Eckardt & Reintjes, 1984; Eimerl, 1987; Milton, 1992). In this case, the three coordinate systems of equations (1.7.3.22) are identical, (X, Y, Z), and the general solution may be written in terms of the Jacobian elliptic function $\mathrm{sn}(m, \alpha)$.

For the simple case of type I, *i.e.* $E_1^\omega(X, Y, Z) = E_2^\omega(X, Y, Z) = E^\omega(X, Y, Z) = E_{tot}^\omega(X, Y, Z)/(2^{1/2})$, the exit second harmonic intensity generated over a length L is given by (Eckardt & Reintjes, 1984)

$$I^{2\omega}(X, Y, L) = I_{tot}^\omega(X, Y, 0) T^{2\omega} T^\omega v_b^2 \mathrm{sn}^2\left[\frac{\Gamma(X, Y)L}{v_b}, v_b^4\right]. \quad (1.7.3.58)$$

Copyright © 2013 International Union of Crystallography

$I^{\omega}_{\rm tot}(X, Y, 0) = 2I^{\omega}(X, Y, 0)$ is the total initial fundamental intensity, $T^{2\omega}$ and T^{ω} are the transmission coefficients,

$$\frac{1}{v_b} = \frac{\Delta s}{4} + \left[1 + \left(\frac{\Delta s}{4}\right)^2\right]^{1/2}$$

with

$$\Delta s = (k^{2\omega} - k^{\omega})/\Gamma$$

and

$$\Gamma(X, Y) = \frac{\omega d_{\rm eff}}{cn^{2\omega}}(T^{\omega})^{1/2}|E^{\omega}_{\rm tot}(X, Y, 0)|. \qquad (1.7.3.59)$$

For the case of phase matching ($k^{\omega} = k^{2\omega}$, $T^{\omega} = T^{2\omega}$), we have $\Delta s = 0$ and $v_b = 1$, and the Jacobian elliptic function sn$(m, 1)$ is equal to tanh(m). Then formula (1.7.3.58) becomes

$$I^{2\omega}(X, Y, L) = I^{\omega}_{\rm tot}(X, Y, 0)(T^{\omega})^2 \tanh^2[\Gamma(X, Y)L], \qquad (1.7.3.60)$$

where $\Gamma(X, Y)$ is given by (1.7.3.59).

The exit fundamental intensity $I^{\omega}(X, Y, L)$ can be established easily from the harmonic intensity (1.7.3.60) according to the Manley–Rowe relations (1.7.2.40), *i.e.*

$$I^{\omega}(X, Y, L) = I^{\omega}_{\rm tot}(X, Y, 0)(T^{\omega})^2 {\rm sech}^2[\Gamma(X, Y)L]. \qquad (1.7.3.61)$$

For small ΓL, the functions $\tanh^2(\Gamma L) \simeq \Gamma^2 L^2$ and ${\rm sn}^2[(\Gamma L/v_b), v_b^4] \simeq \sin^2(\Gamma L/v_b)$ with $v_b \simeq 2/\Delta s$.

The first consequence of formulae (1.7.3.58)–(1.7.3.59) is that the various acceptance bandwidths decrease with increasing ΓL. This fact is important in relation to all the acceptances but in particular for the thermal and angular ones. Indeed, high efficiencies are often reached with high power, which can lead to an important heating due to absorption. Furthermore, the divergence of the beams, even small, creates a significant dephasing: in this case, and even for a propagation along a phase-matching direction, formula (1.7.3.60) is not valid and may be replaced by (1.7.3.58) where $k(2\omega) - k(\omega)$ is considered as the 'average' mismatch of a parallel beam.

In fact, there always exists a residual mismatch due to the divergence of real beams, even if not focused, which forbids asymptotically reaching a 100% conversion efficiency: $I^{2\omega}(L)$ increases as a function of ΓL until a maximum value has been reached and then decreases; $I^{2\omega}(L)$ will continue to rise and fall as ΓL is increased because of the periodic nature of the Jacobian elliptic sine function. Thus the maximum of the conversion efficiency is reached for a particular value $(\Gamma L)_{\rm opt}$. The determination of $(\Gamma L)_{\rm opt}$ by numerical computation allows us to define the optimum incident fundamental intensity $I^{\omega}_{\rm opt}$ for a given phase-matching direction, characterized by K, and a given crystal length L.

The crystal length must be optimized in order to work with an incident intensity $I^{\omega}_{\rm opt}$ smaller than the damage threshold intensity $I^{\omega}_{\rm dam}$ of the nonlinear crystal, given in Section 1.7.5 for the main materials.

Formula (1.7.3.57) is established for type I. For type II, the second harmonic intensity is also an sn^2 function where the

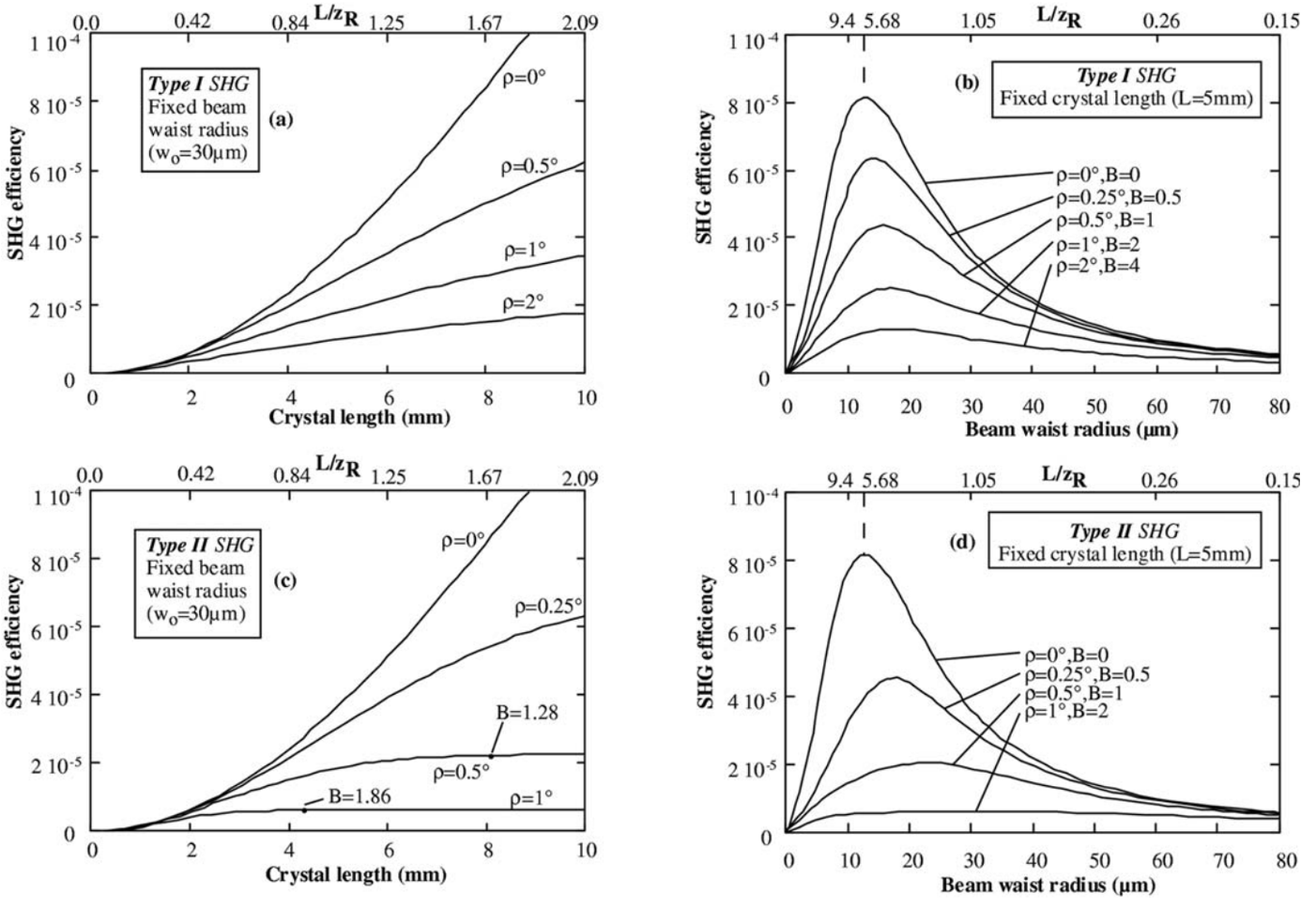

Fig. 1.7.3.14. Type-I and -II conversion efficiencies calculated as a function of L/z_R for different typical walk-off angles ρ: (*a*) and (*c*) correspond to a fixed focusing condition (w_o = 30 μm); the curves (*b*) and (*d*) are plotted for a constant crystal length (L = 5 mm); all the calculations are performed with the same effective coefficient ($d_{\rm eff}$ = 1 pm V^{-1}), refractive indices ($n_3^{2\omega}n_1^{\omega}n_2^{\omega} = 5.83$) and fundamental power [$P_{\omega}(0 = 1$ W]. B is the walk-off parameter defined in the text (Fève & Zondy, 1996).

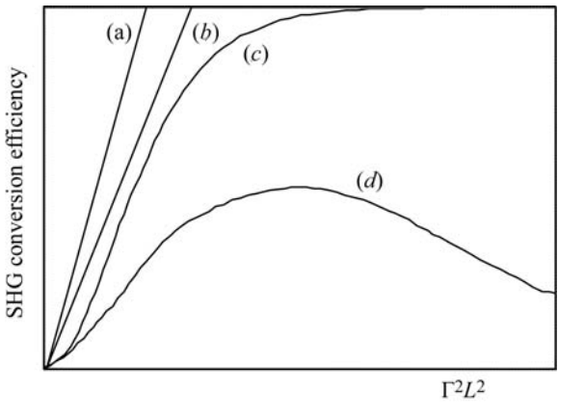

Fig. 1.7.3.15. Schematic SHG conversion efficiency for different situations of pump depletion and dephasing. (*a*) No depletion, no dephasing, $\eta = \Gamma^2 L^2$; (*b*) no depletion with constant dephasing δ, $\eta = \Gamma^2 L^2 \sin c^2 \delta$; (*c*) depletion without dephasing, $\eta = \tanh^2(\Gamma L)$; (*d*) depletion and dephasing, $\eta = \eta_m \mathrm{sn}^2(\Gamma L/v_b, v_b^4)$.

intensities of the two fundamental beams $I_1^\omega(X, Y, 0)$ and $I_2^\omega(X, Y, 0)$, which are not necessarily equal, are taken into account (Eimerl, 1987): the $\tanh^2$ function is valid only if perfect phase matching is achieved and if $I_1^\omega(X, Y, 0) = I_2^\omega(X, Y, 0)$, these conditions being never satisfied in real cases.

The situations described above are summarized in Fig. 1.7.3.15.

We give the example of type-II SHG experiments performed with a 10 Hz injection-seeded single-longitudinal-mode ($N = 1$) 1064 nm Nd:YAG (Spectra-Physics DCR-2A-10) laser equipped with super Gaussian mirrors; the pulse is 10 ns in duration and is near a Gaussian single-transverse mode, the beam radius is 4 mm, non-focused and polarized at $\pi/4$ to the principal axes of a 10 mm long KTP crystal ($L\delta\theta$ = 15 mrad cm, $L\delta\varphi$ = 100 mrad cm). The fundamental energy increases from 78 mJ (62 MW cm^{-2}) to 590 mJ (470 MW cm^{-2}), which correponds to the damage of the exit surface of the crystal; for each experiment, the crystal was rotated in order to obtain the maximum conversion efficiency. The peak power SHG conversion efficiency is estimated from the measured energy conversion efficiency multiplied by the ratio between the fundamental and harmonic pulse duration ($\tau_\omega/\tau_{2\omega} = 2^{1/2}$). It increases from 50% at 63 MW cm^{-2} to a maximum value of 85% at 200 MW cm^{-2} and decreases for higher intensities, reaching 50% at 470 MW cm^{-2} (Boulanger, Fejer *et al.*, 1994).

The integration of the intensity profiles (1.7.3.58) and (1.7.3.60) is obvious in the case of incident fundamental beams with a flat energy distribution (1.7.3.36). In this case, the fundamental and harmonic beams inside the crystal have the same profile and radius as the incident beam. Thus the powers are obtained from formulae (1.7.3.58) and (1.7.3.60) by expressing the intensity and electric field modulus as a function of the power, which is given by (1.7.3.38) with $m = 1$.

For a Gaussian incident fundamental beam, (1.7.3.37), the fundamental and harmonic beams are not Gaussian (Eckardt & Reintjes, 1984; Pliszka & Banerjee, 1993).

All the previous intensities are the peak values in the case of pulsed beams. The relation between average and peak powers, and then SHG efficiencies, is much more complicated than the ratio $\tau^{2\omega}/\tau^\omega$ of the undepleted case.

1.7.3.3.2.4. *Resonant SHG*

When the single-pass conversion efficiency SHG is too low, with c.w. lasers for example, it is possible to put the nonlinear crystal in a Fabry–Perot cavity external to the pump laser or directly inside the pump laser cavity, as shown in Figs. 1.7.3.6(*b*) and (*c*). The second solution, described later, is generally used because the available internal pump intensity is much larger.

We first recall some basic and simplified results of laser cavity theory without a nonlinear medium. We consider a laser in which one mirror is 100% reflecting and the second has a transmission T at the laser pulsation ω. The power within the cavity, $P_{\mathrm{in}}(\omega)$, is evaluated at the steady state by setting the round-trip saturated gain of the laser equal to the sum of all the losses. The output laser cavity, $P_{\mathrm{out}}(\omega)$, is given by (Siegman, 1986)

$$P_{\mathrm{out}}(\omega) = TP_{\mathrm{in}}(\omega)$$

with

$$P_{\mathrm{in}}(\omega) = \frac{2g_o L' - (\gamma + T)}{2S(T + \gamma)}. \qquad (1.7.3.62)$$

L' is the laser medium length, $g_o = \sigma N_o$ is the small-signal gain coefficient per unit length of laser medium, σ is the stimulated-emission cross section, N_o is the population inversion without oscillation, S is a saturation parameter characteristic of the nonlinearity of the laser transition, and $\gamma = \gamma_L = 2\alpha_L L' + \beta$ is the loss coefficient where α_L is the laser material absorption coefficient per unit length and β is another loss coefficient including absorption in the mirrors and scattering in both the laser medium and mirrors. For given g_o, S, α_L, β and L', the output power reaches a maximum value for an optimal transmission coefficient T_{opt} defined by $[\partial P_{\mathrm{out}}(\omega)/\partial T]_{T_{\mathrm{opt}}} = 0$, which gives

$$T_{\mathrm{opt}} = (2g_o L'\gamma)^{1/2} - \gamma. \qquad (1.7.3.63)$$

The maximum output power is then given by

$$P_{\mathrm{out}}^{\max}(\omega) = (1/2S)[(2g_o L')^{1/2} - \gamma^{1/2}]^2. \qquad (1.7.3.64)$$

In an intracavity SHG device, the two cavity mirrors are 100% reflecting at ω but one mirror is perfectly transmitting at 2ω. The presence of the nonlinear medium inside the cavity then leads to losses at ω equal to the round-trip-generated second harmonic (SH) power: half of the SH produced flows in the forward direction and half in the backward direction. Hence the highly transmitting mirror at 2ω is equivalent to a nonlinear transmission coefficient at ω which is equal to twice the single-pass SHG conversion efficiency η_{SHG}.

The fundamental power inside the cavity $P_{\mathrm{in}}(\omega)$ is given at the steady state by setting, for a round trip, the saturated gain equal to the sum of the linear and nonlinear losses. $P_{\mathrm{in}}(\omega)$ is then given by (1.7.3.62), where T and γ are (Geusic *et al.*, 1968; Smith, 1970)

$$T = 2\eta_{\mathrm{SHG}} = [P_{\mathrm{out}}(2\omega)/P_{\mathrm{in}}(\omega)] \qquad (1.7.3.65)$$

and

$$\gamma = \gamma_L + \gamma_{NL}. \qquad (1.7.3.66)$$

η_{SHG} is the single-pass conversion efficiency. γ_L and γ_{NL} are the loss coefficients at ω of the laser medium and of the nonlinear crystal, respectively. L is the nonlinear medium length. The two faces of the nonlinear crystal are assumed to be antireflection-coated at ω.

In the undepleted pump approximation, the backward and forward power generated outside the nonlinear crystal at 2ω is

$$P_{\mathrm{out}}(2\omega) = 2KP_{\mathrm{in}}^2(\omega) \qquad (1.7.3.67)$$

with

$$K = B(L^2/w_o^2)\sin c^2(\Delta kL/2),$$

where

$$B = \frac{32\pi}{\varepsilon_o c}\frac{2N-1}{N}\frac{d_{\mathrm{eff}}^2}{\lambda_\omega^2}\frac{T_3^{2\omega}T_1^\omega T_2^\omega}{n_3^{2\omega}n_1^\omega n_2^\omega} \quad (\mathrm{W}^{-1}).$$